Chemical Evolution of Spheroidal Systems(Proceedings of Japan-France Seminar on Chemical Evolution of Galaxies with Active Star Formation)

著者	YOSHII Yuzuru
journal or publication title	The science reports of the Tohoku University. Ser. 8, Physics and astronomy
volume	7
number	3
page range	371-380
year	1987-03-20
URL	http://hdl.handle.net/10097/25627

Proceedings of Japan-France Seminar on Chemical Evolution of Galaxies

Chemical Evolution of Spheroidal Systems

Yuzuru YOSHII
Tokyo Astronomical Observatory, University of Tokyo
Mitaka, Tokyo 181, Japan

A model of chemical evolution for spheroidal systems is constructed assuming a relation between binding energy and mass of a system $\Omega_G \propto M_G^{1.45}$ and a universal IMF of stars $dn/d\log m \propto m^{-0.95}$. Taking into account the effect of stopping the star formation due to gas removal by a galactic wind, we successfully reproduced the chemical and structural properties of gE galaxies, dE galaxies, and globular clusters. The average metallicity of stars in a system declines from gEs through dEs monotonically, while the galactic mass loss expands dEs most significantly among others, causing the distinct sequences of gEs, dEs, and globulars in the diameter-surface brightness diagram. It is suggested that all the spheroidal systems were formed as a one-parameter family of mass.

Keywords: Chemical evolution, gE galaxies, dE galaxies, globular clusters.

1. Introduction

Luminosities of gE galaxies are correlated with their overall structural quantities[1),2)] . The luminosity-velocity-diameter relations defined by gEs are extended down to much fainter and smaller globular clusters[3)] . If the systems are in dynamical equilibrium, such relations stem from a single relation between binding energy Ω_G and mass M_G of the system[4)] :

$$\Omega_G = 1.66\ 10^{60} M_{12}^{\ \eta} \text{ ergs} \qquad (\eta=1.45) \quad , \tag{1}$$

where M_{12} is the mass M_G in units of $10^{12}M_\odot$. However, dE galaxies are found to have much lower surface brightnesses and larger diameters than predicted[5),6),7)] . Especially, Kormendy[6)] demonstrated that there is no common relationship for all the spheroidal systems despite similarity of their morphological appearence.

Alternatively, the integrated colors of gEs become progressively red as the absolute magnitude decreases[8),9)]. This relation for gEs is extended smoothly down to dEs[10),11)], and further to extremely metal-poor globular clusters[12)]. Since the tight relation between metallicity and magnitude is observed from gEs to dEs[13),14)], the luminosity-color-metallicity relations suggest that there is a common relationship for the spheroidal systems.

From either structural or chemical properties of spheroidal systems, we are led to different conclusions contrary to each other. This apparent inconsistency reminds us of a supernovae-driven wind model of chemical evolution which allows the expansion of a system due to gas removal by a galactic wind[15),16),17)]. Applying the wind model to spheroidal systems of gEs, dEs, and globular clusters, we show that all their properties may be originated from a common relation between binding energy and mass at birth of the systems.

2. Supernovae-Driven Wind Model

Given the IMF $\varphi(m)$ [$\equiv$dn/dlog$m$] and the SFR $C(t)$, the evolutions of the fractional gas mass $f_g(t)$ and the metal abundance $Z_g(t)$ in the gas are determined by the following equations:

$$\frac{df_g}{dt} = -C(t)+\int_{\max(m_l,m_t)}^{m_u} R(m)\varphi(m)C(t-t_m)dm \quad , \tag{2}$$

and

$$\frac{d(f_gZ_g)}{dt} = -C(t)Z_g(t)+\int_{\max(m_l,m_t)}^{m_u} \{Q_z(m)+Z_g(t-t_m)\,[R(m)-Q_z(m)]\}\,\varphi(m)C(t-t_m)dm \quad , \tag{3}$$

respectively, where $R(m)$ is the fractional mass ejected from the stars with mass m, and $Q_z(m)$ is that of metals newly synthesized in stars with mass m and then ejected into the interstellar medium, t_m is the lifetime of stars with mass m, and m_t is the turnoff mass for which $t_m=t$. These differential Eqs.(2) and (3) are numerically integrated with the initial values of $f_g(0)=1$ and $Z_g(0)=0$ up to t_G=15Gyr.

The IMF is assumed to be time-invarient and to have a power-law mass spectrum:

$$\varphi(m) = \frac{(\mu-1)m_l^{\mu-1}}{1-(m_l/m_u)^{\mu-1}}\, m^{-\mu} \qquad (m_l\leq m\leq m_u) \quad , \tag{4}$$

where the lower and upper mass limits are taken to be $m_l=0.05M_\odot$ and $m_u=60M_\odot$, respectively. Introducing the cutoff time t_{GW} of star formation due to gas removal by a galactic wind, we adopt the SFR as

$$C(t) = \nu f_g \quad (t<t_{GW})$$
$$= 0 \quad (t\geqq t_{GW}), \tag{5}$$

where ν is a constant rate coefficient and the cutoff time t_{GW} will be defined below. The parameters ν and μ are chosen such that the model for $M_G=10^{12}M_\odot$ reproduces the absolute magnitude M_V=-23 mag and the *UBVRIJKL* colors at t_G=15Gyr. The values derived here are ν/ν_0=45 and μ=0.95[19], where $\nu_0=6.08\ 10^{-18}s^{-1}$ is appropriate for the SFR in the solar neighborhood. We assume that the systems with other initial masses have the same age t_G=15Gyr and the same IMF with μ=0.95. Assuming that the relation (1) represents the initial conditions with which global star formation takes place in protogalaxies, we evaluate the value of ν for $M_G\neq10^{12}M_\odot$. The SFR may depend on M_G through a certain combination of structural quantities, because it may be determined by comaparing the time scale of star formation to the shorter time between the free-fall time and the collision time of fragmentary clumps[18], i.e.,

$$\nu/\nu_0 = 7.13\ 10^2(M_G/M_\odot)^{2\eta-3} \quad (M_G\geqq4.1\text{x}10^7M_\odot)$$
$$= 3.68\ 10^4(M_G/M_\odot)^{(3\eta-5)/2} \quad (M_G<4.1\text{x}10^7M_\odot) \quad , \tag{6}$$

provided that ν/ν_0=45 for $M_G=10^{12}M_\odot$.

The thermal energy in a galaxy is given by

$$E_{th}(t) = 0 \quad (t<t_{msn,u})$$
$$= \int_{\max(m_{sn,l},m_t)}^{m_{sn,u}} dm \int_0^{t-t_m} \varepsilon(t-t_m-t')(M_G/m)\varphi(m)C(t')dt' \quad (t\geqq t_{msn,u}) \quad , \tag{7}$$

which is compared with the binding energy of the gas

$$\Omega_g(t) = \Omega_G f_g(t)[2-f_g(t)] \quad , \tag{8}$$

where $m_{sn,l}=3M_\odot$, $m_{sn,u}=m_u(=60M_\odot)$, and $\varepsilon(t)$ is the thermal energy content in the interior of a SNR. We show in Fig.1 the evolutions of E_{th} and Ω_g for three cases of $M_G=10^6, 10^9$, and $10^{12}M_\odot$. As shown in this figure, E_{th} begines to increase after the lifetime of the most massive stars ($m_{sn,u}=60M_\odot$), while Ω_g decreases from the initial value Ω_G. Then, they become equal to each other at time t_{GW} satisfying $E_{th}(t_{GW})=\Omega_g(t_{GW})$. We assume that, when E_{th} exceeds Ω_g at $t>t_{GW}$, the residual gas in a galaxy is driven out by a galactic wind and the formation of new stars is stopped.

Since the SFR coefficient ν which is proportional to the negative power of M_G gives a lower rate of SN explosions in the early era of larger systems, a galactic wind occurs later and chemical evolution proceeds more effectively in larger systems, as shown in Fig.2. On the other hand, the fractional mass f_{GW} of gas which remains at t_{GW} shows a marked dependence on M_G, as shown in Fig.3. In case of $M_G\sim10^{11-12}M_\odot$, the epoch of occurrence of a wind is delayed

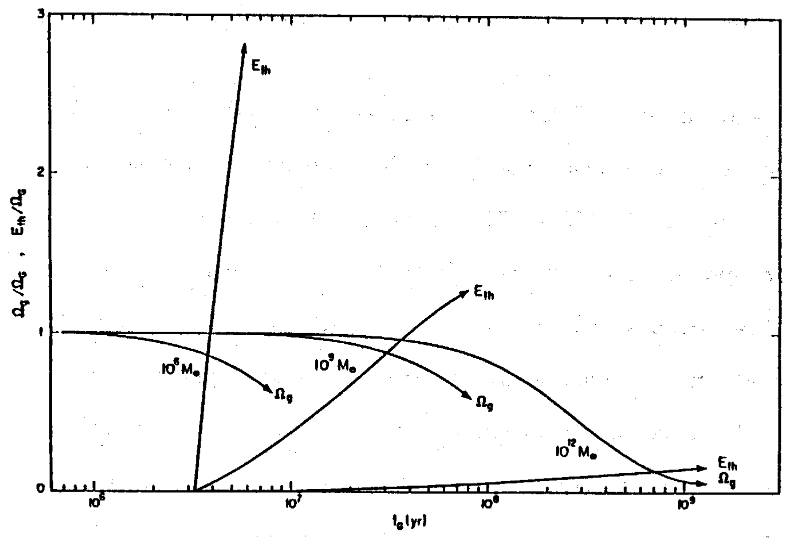

Fig.1. Evolutions of thermal energy E_{th} and binding energy of the residual gas Ω_g. The energies are relative to the initial binding energy Ω_G of the system.

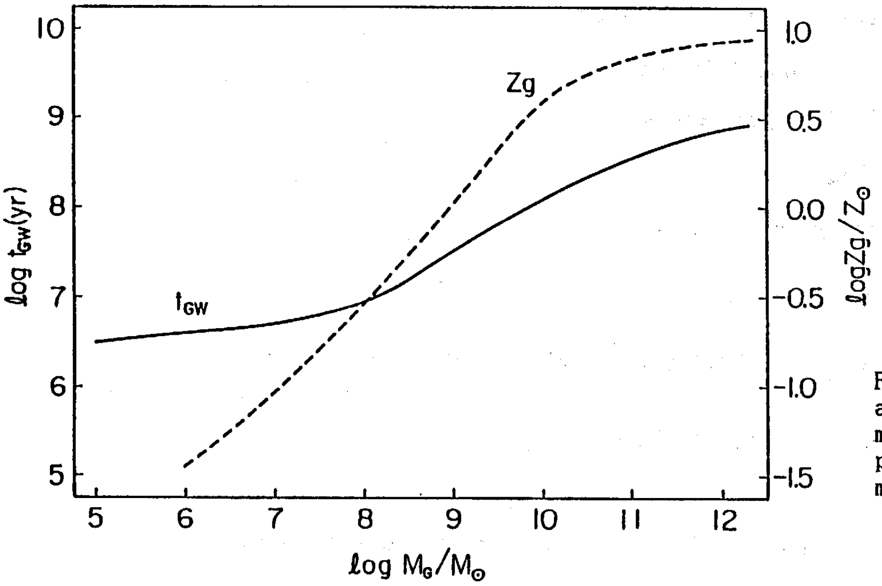

Fig.2. Epoch of occurence of a galactic wind t_{GW} and metallicity of residual gas Z_g plotted against the initial mass M_G of the system.

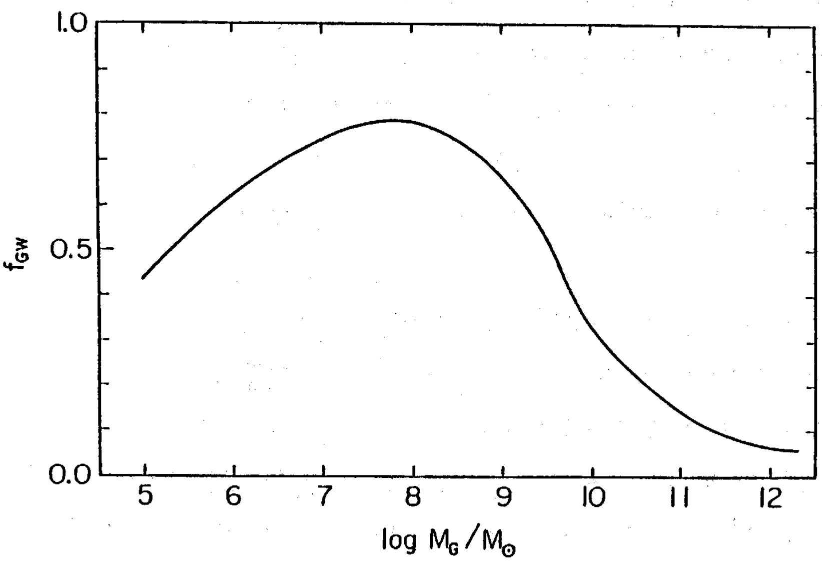

Fig.3. Fractional mass of remaining gas at the epoch of occurrence of a galactic wind plotted against the initial mass M_G of the system.

considerably until almost all the gas turns into stars and the binding energy of the gas becomes very small (Fig.1). In the other extreme case of $M_G \sim 10^{5-6} M_\odot$, most gas is used up at considerably high SFR before massive stars of the earliest generation explode. For this reason, only dEs with intermediate mass between gEs and globular clusters can lose more than half of their initial mass.

We here consider the fate of the mass-losing systems, by comparing the time scale of mass loss t_{loss} to the time scale t_{cross} in which a star crosses the system at the virial velocity of the system. The mass loss occurs in a galactic wind when the sound velocity of the heated gas exceeds the escape velocity[15]. Figure 1 indicates that the thermal energy E_{th} for $M_G=10^6 M_\odot$ grows rapidly exceeding Ω_g by more than an order of magnitude soon after $t=t_{GW}$ and hence the gas begines to escape from the system at the sound velocity enormously larger than the virial velocity, i.e., $t_{loss} \ll t_{cross}$. Therefore, such a small system favors the condition for rapid removal of the gas. In the other cases of $M_G=10^9$ and $10^{12} M_\odot$, E_{th} remains slightly larger than Ω_g even after $t=t_{GW}$ so that the sound velocity is of the same order of magnitude as the virial velocity, i.e., $t_{loss} \sim t_{cross}$. This suggests that the heated gas begins to overflow the system continuously and the stellar system expands almost in the same time scale as the gas is lost. Therefore, such large systems favor, more or less, the condition for slow removal of the gas. Since it is not easy to deduce dynamical responce of a system in the condition of $t_{loss} \sim t_{cross}$, we will study two extreme cases of the slow and rapid removal of the gas in this paper.

3. Comparision of the Wind Model with Observations

3.1 Metallicity - Magnitude Relation

The frequency distributions of stellar metallicity for $M_G=10^7$ to $10^{12} M_\odot$ are shown in Fig.4. It is evident from this figure that dEs are composite stellar systems similar to gEs, and that larger systems are composed of stars with higher metallicities. The binding energy of systems with $M_G<10^6 M_\odot$ is so small that a wind occurs as soon as massive stars of the earliest generation explode. Consequently, such systems are expected to have the metallicity with which the first stars were born. In other words, there exists a critical initial mass which devides small systems into dEs and globular clusters. This idea is supported by the obervational fact that globular clusters are composed of stars of single metallicity[20] whereas dEs have spread in stellar metallicities[21),22),23] . Further supportive evidence is that the most massive globular cluster ω Cen exhibits distinct abundance variations[24] .

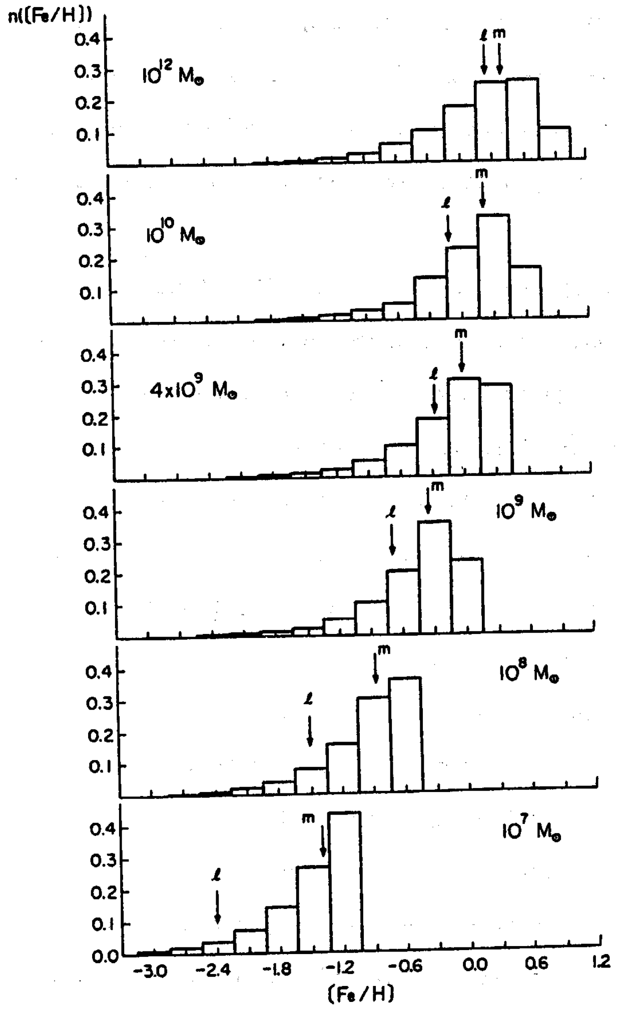

◀ Fig.4. Metallicity distribution of stars in the models of $M_G=10^7$ to $10^{12}M_\odot$. The arrows with m and l indicate the average metallicities $[Fe/H]_m$ and $[Fe/H]_l$ weighted by stellar mass and luminosity, respectively.

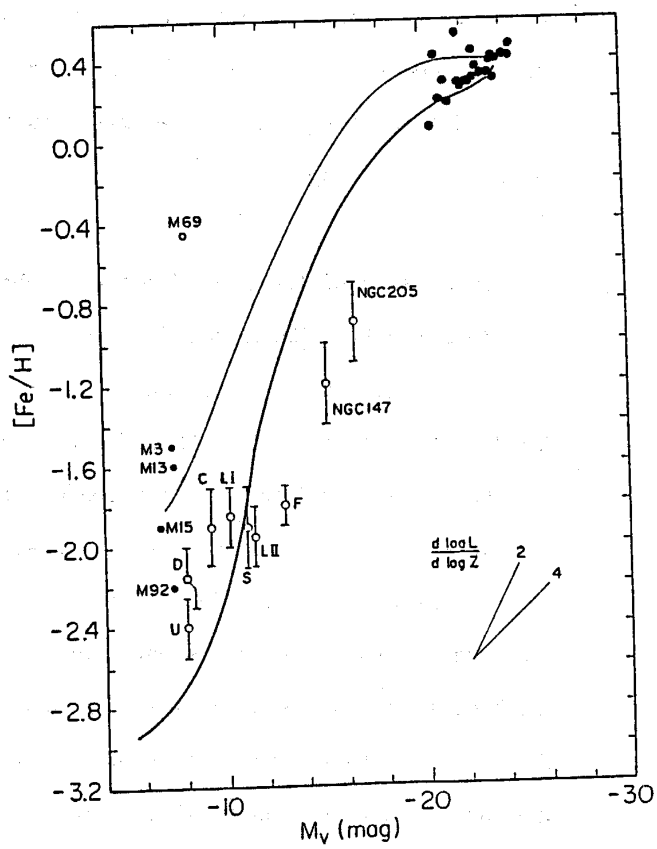

Fig.5. Metallicity versus absolute V-magnitude. The thin and thick lines represent the $[Fe/H]_m$-M_V relation and the $[Fe/H]_l$-M_V relation, respectively. The data of ellipticals, dwarfs, and globular clusters are distinguished by the size of circles. Ellipticals are represented by filled circles of the largest size, and dwarfs by open circles of the intermediate size. Galactic globular clusters in three metallicity ranges of $[Fe/H] \geq -0.7$, $-0.7 > [Fe/H] \geq -1.5$, and $-1.5 > [Fe/H]$ are represented by open, crossed, and filled circles of the smallest size, respectively. Especially, the dwarf spheroidals of Fornax, Sculptor, Carina, Leo I, Leo II, Draco, and Ursa Minor are denoted by the symbols F, S, C, LI, LII, D, and U, respectively. ▶

The metallicity of composite stellar system is characterized by the luminosity-weighted average $[Fe/H]_l$ and the mass-weighted average $[Fe/H]_*$. For the IMF with μ=0.95, the metallicity $[Fe/H]_l$ corresponds to the average metallicity of red giants, while $[Fe/H]_*$ to late dwarfs. The average metallicities defined by $[Fe/H]_l$ and $[Fe/H]_*$ are indicated by arrows in Fig.4. The value of $[Fe/H]_l$ is much lower than $[Fe/H]_*$. The metallicity of a system we observe is weighted significantly by stellar luminosity, i.e., the average metallicity of metal-poor red giants which are most luminous in old stellar systems. Therefore, the observed metallicities should be compared with $[Fe/H]_l$ of the same absolute magnitude.

Figure 5 shows the average metallicity versus the absolute magnitude at t_G=15Gyr. The theoretical $[Fe/H]_l$ -M_V relation is consistent with the data of gEs and dEs. However, the predicted metallicities of globular clusters are smaller than the observed lower limit. If we adopt the initial metallicity of $[Fe/H] \sim -2.5$ or so in the chemical evolution, the faint end of the theoretical $[Fe/H]_l$ -M_V relation shifts up to the region of extremely metal-poor globular clusters. Thus, we may conclude that gEs, dEs, and globular clusters obey a monotonical sequence of their mass, and that the globular clusters now observed with $[Fe/H] > -2$ were formed from chemically processed gas, somehow during the early collapse of the Galaxy[24) . The model predicts the metallicity $[Fe/H]_l$ about three times larger than those of NGC147 and NGC205. It is pointed out, however, that the metallicities of these galaxies should be regarded as lower limits because they are based on red giants in the outer halo of the galaxies, not in the central regions[25) .

3.2 Diameter and Surface Brightness Diagram

Expansion of a system increases the diameter D and lowers the surface brightness SB. Since the time scale of expansion is much shorter than the time scale of luminosity evolution, the evolutionary track in the D-SB diagram is characterised by the slope of $\Delta SB/\Delta \log D$ = 5. The theoretical D-SB relations realized after slow and rapid removals of the gas are shown in Fig.6. The thin lines with arrows represent the evolutionary tracks which connect the initial state of a system to the present-day state predicted by the wind model. It is clear that, in either slow or rapid removal, the region to the right of the terminal D-SB line is a forbidden area, because the remaining gas is assumed to be lost completely from the system in this paper.

The terminal D-SB line for slow removal is continuous from gEs to globular clusters. On

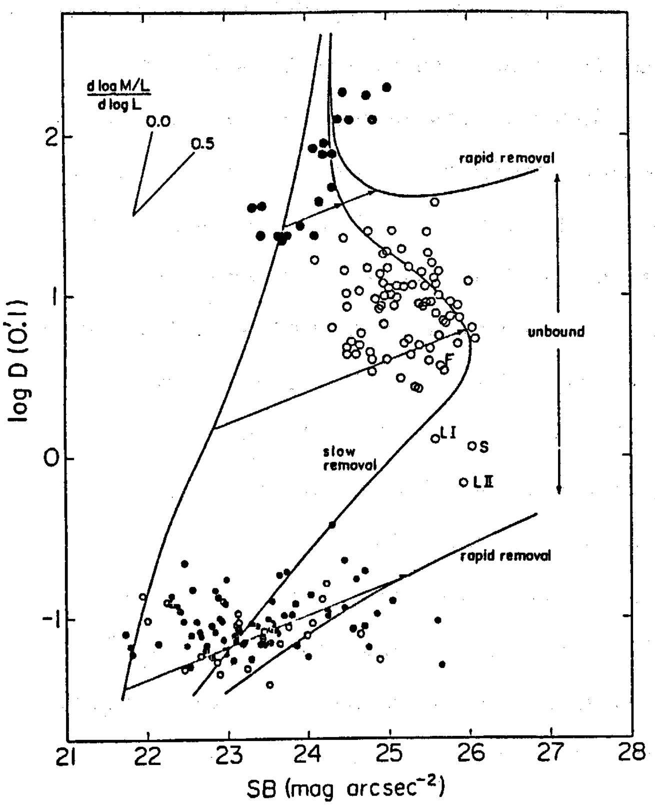

Fig.6. Diameter versus surface brightness. The thick lines are the theoretical *D-SB* relations with and without correcting the effect of expansion of a system. The thin lines with arrows are evolutionary tracks which connect the initial state of a system to the present-day state predicted by the wind model. The symbols of the data are the same as in Fig.5.

the other hand, the terminal *D-SB* line for rapid removal is discontinuous owing to $f_{CV}>0.5$. Galaxies in this region should expand without recovering a new equilibrium state. Thus, the forbidden area for rapid removal covers so large an area in the *D-SB* diagram that most dEs cannot survive.

The observational data of gEs and dEs in Virgo cluster and Galactic globular clusters taken from Ichikawa et al.[7] are also shown in Fig.6, where the globular clusters are located at the distance of Virgo cluster. It is evident from Fig.6 that gEs, dEs, and globular clusters have their own empirical sequences, and that the theoretical *D-SB* relation without the effect of expansion of a system deviates from all these empirical sequences.

The empirical gE sequence has the slope $\Delta SB/\Delta \log D \sim 2$ [26),27)] which is larger than that predicted by the wind model. This discrepancy is attributed to the fact that the slope is sensitive to the mass-to-luminosity ratio M/L_B. Although chemical evolution gives a constant M/L_B ratio for gEs[19], there is an observational trend that the M/L_B ratio increases toward bright gEs[2),29),30)]. Introducing the additional mass in such a way as $M/L_B \propto L_B^{0.5}$, we can reproduce the empirical gE sequence.

Most dEs reside in the forbidden area for rapid removal, but within the permitted area for slow removal. Therefore, as predicted by the wind model (see Section 2), the observations are consistent with the slow removal. On the other hand, most globular clusters reside within the permitted area for rapid removal. The fact that the clusters are distributed along a sequence with a characteristic slope of $\Delta SB/\Delta \log D \sim 5$ suggests that the clusters expand indeed. It may be dangerous, however, to conclude that globular clusters expand due to rapid removal of the gas by a galactic wind, because the gas can also be stripped when the clusters pass through the galactic disk, or low-mass stars are lost to form the extended envelopes through dynamical evolution of the clusters. Here, we should note that the distribution of the clusters in the *D-SB* diagram does not depend on their metallicity range. This suggests that globular clusters are always formed under similar initial conditions during the early collapse of the Galaxy.

4. Summary and Discussion

A supernovae-driven wind model for spheroidal systems is constructed under a relation between binding energy and mass of the system $\Omega_G \propto M_G^{1.45}$ and a universal IMF of stars $dn/d\log m \propto m^{-0.95}$. Simple argument indicates that the relation $\Omega_G \propto M_G^{1.45}$ gives the SFR per unit mass which is proportional to a negative power of M_G. Thereby, a galactic wind occurs later and metal enrichment proceeds more effectively in larger galaxies. The fractional mass of gas which remains to be lost in a wind does not show a monotonical trend with M_G; the fraction gives a maximum value at $M_G \sim 10^{7-9} M_\odot$, while it decreases toward both smaller and larger M_G. The expansion of mass-losing systems does not violate the monotonical trend of integrated photometric quantities with the mass of the systems, but it changes the structural quantities most significantly for dEs. Successful reproduction of the observed trends strongly suggests a possibility that all the spheroidal systems over the range of 10^7 in mass are formed as a one-parameter family of mass.

Contrary to our conclusion, previous authors[31),32)] pointed out that the relation $M_G \propto R_G^{1.8}$ (equivalently $\Omega_G \propto M_G^{1.45}$) cannot be compatible with the observed steep decline of metallicity from gEs to dEs in Local group. To lower the effective yield of metallicity in chemical evolution, Vader[31)] proposed the model of metal-enhanced galactic wind which carries away a large fraction of metal production by SNs. Dekel & Silk[32)] proposed the model of mass loss with no expansion of systems in dominant halos, assuming the relation $M_G \propto R_G^{2.5}$ presently observed for only dEs. This relation gives lower mass density and hence lower efficiency of chemical evolution toward faint dEs than our relation $M_G \propto R_G^{1.8}$ predicts. However, we should note that dEs are composite stellar systems similar to gEs. The observed metallicity of such composite systems should be compared with the luminosity-weighted average metallicity $[Fe/H]_l$ because the quantities of metal-poor and luminous red giants are weighted significantly in observations[19]. The currently used mass-weighted metallicity $[Fe/H]_m$ is always larger than the luminosity-weighted metallicity $[Fe/H]_l$ and the difference becomes monotonically large for small and metal-poor composite systems, in particular, amounting up to a factor of 1.0 dex for dEs in Local group. Consequently, the previous criticism is not fatal to the simple wind model of mass loss.

Acknowlegements: The author thanks N. Arimoto for discussions. This work was supported in part by Scientific Research Funds of Ministry of Education, Science, and Culture of Japan (No.60740129).

References

1) R.A. Fish: Astrophys. J. 139 (1964) 284.
2) S.M. Faber, & R.E. Jackson: Astrophys. J. 204 (1976) 668.
3) G. Illingworth: Astrophys. J. 204 (1976) 73.
4) M. Saito: Publ. Astron. Soc. Japan 31 (1979) 181.
5) B. Binggeli, A. Sandage, & M. Tarenghi: Astron. J. 89 (1984) 64.
6) J. Kormendy: Astrophys. J. 295 (1985) 73.
7) S. Ichikawa, K. Wakamatsu, & S. Okamura: Astrophys. J. Suppl. 60 (1986) 475.
8) S.M. Faber: Astrophys. J. 179 (1973) 731.
9) N. Visvanathan, & A. Sandage: Astrophys. J. 216 (1977) 214.
10) N. Caldwell: Astron. J. 88 (1983) 804.
11) H. Zinnecker, R.D. Cannon, J.G. Hawarden, & H.T. MacGillivary: in *Virgo Cluster of Galaxies*, ed. O.-G. Richter, & B. Binggeli (ESO: Garching) (1985) 135.
12) J.A. Frogel, S.E. Persson, M. Aaronson, & K. Matthews: Astrophys. J. 220 (1978) 75.
13) J.R. Mould: Publ. Astron. Soc. Pacific 96 (1984) 773.
14) G.H. Smith: Publ. Astron. Soc. Pacific 97 (1985) 1058.
15) R.B. Larson: M.N.R.A.S. 169 (1974) 229.
16) S. Ikeuchi: Prog. Theore. Phys. 58 (1977) 1742.
17) M. Saito: Publ. Astron. Soc. Japan 31 (1979) 193.
18) Y. Yoshii, & H. Saio: Astrophys. J. 295 (1985) 521
19) N. Arimoto, & Y. Yoshii: Astron. Astrophys. 173 (1987) 23
20) A. Sandage, & B. Katem: Astrophys. J. 215 (1977) 62.
21) J.R. Mould, J. Kristian, & G.S. Da Costa: Astrophys. J. 270 (1983) 471.
22) J.R. Mould, J. Kristian, & G.S. Da Costa: Astrophys. J. 278 (1984) 575.
23) G.S. Da Costa: Astrophys. J. 285 (1984) 483.
24) R.P. Kraft: in *Globular Clusters*, ed. D. Hanes, & B. Maeder (Cambridge University Press: Cambridge) (1980) 87.
25) J.E. Gunn: in *Globular Clusters*, ed. D. Hanes, & B. Maeder (Cambridge University Press: Cambridge) (1980) 301.
26) M. Aaronson: in *Star Forming Dwarf Galaxies and Related Objects*, ed. D. Kunth, T.X. Thuan, & J. Tran Thank Van (Editions Frontieres: Paris) (1986) 125.
27) J. Kormendy: Astrophys. J. 214 (1977) 359.
28) K. Kodaira, S. Okamura, & M. Watanabe: Astrophys. J. Lett. 266 (1983) L21.
29) R. Michard: Astron. Astrophys. 121 (1983) 313.
30) J.P. Vader: Astrophys. J., 306 (1986) 390.
31) J.P. Vader: Astrophys. J., 305 (1986) 669.
32) A. Dekel, & J. Silk: Astrophys. J. 303 (1986) 39.